Geodesy and Geodynamics 14 (2023) 265–274

Contents lists available at ScienceDirect

Geodesy and Geodynamics

journal homepage: http://www.keaipublishing.com/geog

# Performance of GPS and IMU sensor fusion using unscented Kalman filter for precise i-Boat navigation in infinite wide waters

Mokhamad Nur Cahyadi [a, b, *], Tahiyatul Asfihani [c], Ronny Mardiyanto [d], Risa Erfianti [a]

[a] Department of Geomatics Engineering, Institut Teknologi Sepuluh Nopember, Surabaya 60111, Indonesia
[b] Research Center of Marine and Earth Science-Technology, Directorate of Research and Community Service, Institut Teknologi Sepuluh Nopember, Surabaya 60111, Indonesia
[c] Department of Mathematics, Institut Teknologi Sepuluh Nopember, Surabaya 60111, Indonesia
[d] Department of Electrical Engineering, Institut Teknologi Sepuluh Nopember, Surabaya 60111, Indonesia

ARTICLE INFO

*Article history:*
Received 27 August 2022
Accepted 1 November 2022
Available online 9 December 2022

*Keywords:*
GPS
IMU
Fusion sensor
6 DOF USV motion
Unscented Kalman filter

ABSTRACT

The Unmanned Surface Vehicle (USV) navigation system needs an accurate, firm, and reliable performance to avoid obstacles, as well as carry out automatic movements during missions. The Global Positioning System (GPS) is often used in these systems to provide absolute position information. However, the GPS measurements are affected by external conditions such as atmospheric bias and multipath effects. This leads to the inability of the stand-alone GPS to provide accurate positioning for the USV systems. One of the solutions to correct the errors of this sensor is by conducting GPS and Inertial Measurement Unit (IMU) fusion. The IMU sensor is complementary to the GPS and not affected by external conditions. However, it accumulates noise as time elapses. Therefore, this study aims to determine the fusion of the GPS and IMU sensors for the i-Boat navigation system, which is a USV developed by Institut Teknologi Sepuluh Nopember (ITS) Surabaya. Using the Unscented Kalman filter (UKF), sensor fusion was carried out based on the state equation defined by the dynamic and kinematic mathematical model of ship motion in 6 degrees of freedom. Then the performance of this model was tested through several simulations using different combinations of attitude measurement data. Two scenarios were conducted in the simulations: attitude measurement inclusion and exclusion (Scenarios I and II, respectively). The results showed that the position estimation in Scenario II was better than in Scenario I, with the Root Mean Square Error (RMSE) value of 0.062 m. Further simulations showed that the presence of attitude measurement data caused a decrease in the fusion accuracy. The UKF simulation with eight measurement parameters (Scenarios A, B and C) and seven measurement parameters (Scenarios D, E and F), as well as analytical attitude movement, indicated that yaw data had the largest noise accumulation compared to roll and pitch.



## 1. Introduction

The Unmanned Surface Vehicle (USV) has rapidly increased due to its widespread use in several conditions, such as oil and gas exploration, oceanographic data collection, surveillance and reconnaissance, mine countermeasure, and hydrographic, oceanographic, and environmental surveys. A USV system is designed to know its exact location and orientation, as well as to safely navigate any aquatic environment. This indicates that developing high-integrity navigation (localization) systems is critical in autonomous vehicle applications. During the independent movement of the USV performance, the guarantee of robust, accurate, and

* Corresponding author. Department of Geomatics Engineering, Institut Teknologi Sepuluh Nopember, Surabaya 60111, Indonesia.
*E-mail address:* cahyadi@geodesy.its.ac.id (M.N. Cahyadi).

Peer review under responsibility of Institute of Seismology, China Earthquake Administration.

Production and Hosting by Elsevier on behalf of KeAi

https://doi.org/10.1016/j.geog.2022.11.005

reliable navigation is also important [1]. Moreover, a reliable and accurate navigation system is essential for this vehicle to support expected trajectories, even in very dynamic environments. These USV systems generally utilize two sensor types, namely the Global Positioning System (GPS) and the Inertial Measurement Unit (IMU). The GPS has the advantage of producing absolute position and stable accuracy, although influenced by external conditions such as atmospheric bias and multipath effects. Several studies have reportedly implemented various GPS measurement strategies (precise point positioning (PPP) model, real-time kinematic (RTK), or Satellite-Based Augmentation System (SBAS)) to overcome these limitations [2–4]. Meanwhile, the IMU provides accurate attitude measurements unaffected by external conditions, although noise is observed to periodically accumulate [5]. According to P.D. Groves [6], the GPS frequency was generally 10 Hz, which was lower than the IMU at a minimum of 50 Hz, which indicated that IMU recorded more data than GPS in similar periods, subsequently leading to its ability to thoroughly observe USV changes with more intensity.

Based on the advantages and limitations of the complementary GPS and IMU sensors, a multi-sensor fusion was carried out for a more accurate navigation solution, which was conducted by utilizing and mitigating the strengths and weaknesses of each system. The accuracy of sensor fusion also depends on the used data algorithm. Several studies have been conducted based on the estimation of positions from the fusion of GPS and IMU sensors. Using Kalman Filter, the measurements of this fusion improved the position accuracy of static reference points in condensed areas, including areas surrounded by tall buildings or possessing dense canopies. The GPS receivers in these areas were often obstructed, leading to the inability to capture signals from 4 satellite constellations [7]. This study was conducted to determine the accuracy of sensor fusion using the Extended Kalman Filter (EKF) algorithm at static points without considering the degrees of freedom (DOF). The result showed that this fusion provided better measurement accuracy than the stand-alone GPS. Furthermore, Liu et al. [8] studied the fusion of GPS and IMU sensors to strengthen USV navigation in shallow water environments within 3 DOF, considering the motions of the surge, sway, and yaw, respectively. This study applied the Fuzzy Adaptive Kalman Filtering method to the Unscented Kalman Filter (UKF) algorithm. The results showed that the position accuracy increased by 30% compared to conventional UKF. Meanwhile, Guo et al. [9] conducted a study on the integration of Strapdown Inertial Navigation System (SINS) and GPS on surface ships in 4 DOF (considering surge, sway, yaw, roll motions), using three different methods, namely EKF, UKF, and Cubature Kalman Filter (CKF). This indicated that UKF obtained the best results in overcoming gyroscope sensor noise, although it used the dynamic model of the USV movement without considering the kinematic technique.

The sensor fusion of GPS and IMU at 6 DOF is presently very limited since it is a challenge that needs further analysis. The simulated system represents the actual conditions better with the 6 DOF model. Furthermore, the traditional method uses 3 and 4 DOF mathematical models, which are often characterized by several detection parameters, relatively large errors, and insufficient accuracy [10]. However, considering the heave and pitch motion, more accurate modeling with large amplitudes besides the beam sea is allowed [11]. Mathematical modeling at 6 DOF also considers the surge, sway, and yaw ship motions under disturbances induced by wave, wind, and ocean currents. Therefore, this study aims to determine the GPS-IMU sensor fusion on the Intelligent Boat (i-Boat) system developed by the Directorate of Research and Community Service of Institut Teknologi Sepuluh Nopember (DRPM ITS). This vehicle was designed to carry out several roles, such as shipping safety, logistics fulfillment, as well as defense and security functions. USV positioning accuracy is critical in shipping safety missions, because the USV sends information in the form of position coordinates if a drowning victim is found or the location of a ship accident is found. With accurate position information, mitigation efforts on ship accidents can be carried out more efficiently.

The novelty of this study is based on the following: 1. Sensor fusion is carried out based on the 6 DOF USV motions represented by the dynamic and kinematic model; 2. The mathematic model is constructed with the assumption that i-Boat operates in wide waters by differentiating the working forces on USV; 3. The performance of the UKF algorithm is tested by modifying the combination of measurement data.

This research proposes the application of 6 DOF modeling on USV sensor fusion instead of developing the novel filter algorithm. This study uses UKF as a filter algorithm. However, previous studies have developed more novel filtering methods, such as multi-rate strong tracking and self-learning square-root cubature Kalman filter [12,13], which can estimate the system covariance adaptively and provide navigation solutions continuously even during long-term GPS outages. Liu et al. [8] also showed that adaptive UKF outperforms the standard UKF. However, this study prefers the standard UKF method because it is suitable for solving highly nonlinear models with a relatively lower computational load [9].

In this study, the utilization of UKF caused an unstable problem when the covariance matrix (should theoretically be positive-definite) became negative, subsequently leading to the usage of the nearest symmetric and positive definite (nearest SPD) decomposition. The UKF also capitalizes on the nonlinear model in the Kalman gain computation to realize simple, high-precision and rapid convergence. Moreover, it theoretically leads to better performances than the other nonlinear Kalman Filter algorithms [9]. Two of the UKF simulations are Scenarios I and II, which are used to identify the algorithm performance in accurately providing i-Boat navigation estimation.

## 2. Sensor measurement experiment

The data used in this study were obtained from an i-Boat experiment during the initial launching event of the vehicle at Galangan Kapal Madura, geographically located at 7.171562° S and 112.7174701° E. In the experiment, the length of the trajectory was 3320 m. Moreover, data were recorded by the GPS and IMU sensors designed at the stand-frame top and steering front, respectively (Fig. 1). During the launching event, the environmental conditions and the i-Boat movement were subsequently recorded in a video accessed on the following link https://youtu.be/uPy6DD1_mDY.

### 2.1. Design of GPS and IMU measurement

The GPS used in this USV had an RTK mode accuracy of approximately 0.025 m, with the ability to receive signals from several satellite constellations, such as L1C/A, GLONASS L1OF, and BeiDou B1I. The type of receiver used by this sensor was U-Blox M8 high precision Global Navigation Satellite System (GNSS) modules (M8P), which had a data update frequency of 8 Hz. The data obtained from the GPS were the coordinates of the i-Boat position on the latitude, longitude, and height within the World Geodetic System (WGS-84) ellipsoidal model. Before performing the sensor

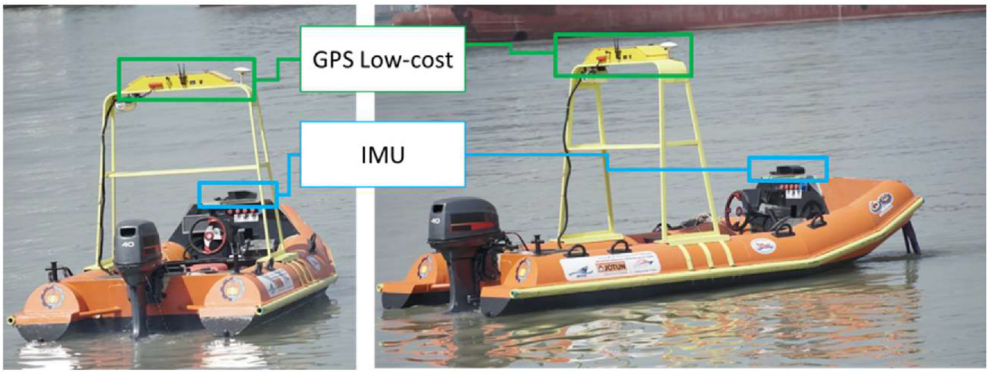


**Fig. 1.** USV i-Boat using low-cost GPS and IMU as an autonomous navigation system.

fusion, these coordinates were projected into the Universal Transverse Mercator (UTM) Zone 49S system. Meanwhile, the information obtained from the IMU sensor was separated into two, namely the accelerometer and gyroscope data, which had output rate specifications between 4–4000 Hz and 4–8000 Hz, respectively. The accelerometer data was the acceleration in the *x*, *y*, and *z* axes (mGal), while that of the gyroscope was the angular (radian)and oblique rate (rad/s). The sensor error characteristics of IMU are presented in Table 1.

The IMU used in this study could integrate the data of acceleration and angular rate, leading to oblique and velocity parameters. This integration was carried out according to the scheme in Fig. 2.

Based on this study, the raw data of the GPS pseudo and Doppler measurements were measured at 2 Hz, and the IMU raw data were measured at a frequency up to 4000 Hz for the accelerometer sensor and 8000 Hz for the gyroscope sensor as the specification shown in Table 2. However, the data recorded at 4 Hz were measured to optimize the memory during the experiment. The data used in the sensor fusion process are in the following format.

### 2.2. Filtering method

The sensor fusion carried out in this study was a loosely coupled integration with the assumption that no error was observed in the GPS signals. This fusion was performed using the UKF algorithm, which consisted of 2 stages, namely the prediction and estimation/correction phases. Furthermore, the data from both the GPS and IMU sensors were integrated based on the 6 DOF USV motions, which contained the kinematic and dynamic models. The kinematic technique represented the motion of an object without considering the causes. Therefore, it is essential to consider the position, velocity, and acceleration in this specific model. Table 3 shows the 6 DOF kinematic models of the ship [15].

In this model, the dot notation states the derivation of time; *x*, *y*, and *z* are the position of the surge, sway, and heave motions, respectively; $\phi$, $\theta$, and $\psi$ are the angle of roll, pitch, and yaw motions, respectively; *u, v,* and *w* are the linear velocity in the surge, sway, and heave motions, respectively; *p, q,* and *r* are the angular velocity in roll, pitch, and yaw motions, respectively.

However, the dynamic model was formulated by considering the forces affecting the stability of the ship. Assuming that the USV operated in infinite wide waters and separated the considered ship forces, the dynamic model is shown in Table 4 [10]:

In this model, $m$ is mass; $m_x, m_y,$ and $m_z$ are added mass coefficients; $I_x, I_y,$ and $I_z$ are the inertia of moments; $J_{xx}, J_{yy},$ and $J_{zz}$ are added moment coefficients; $X, Y,$ and $Z$ are the force of surge, sway, and heave motions, respectively; $K, M,$ and $N$ are the moments in roll, pitch, and yaw motions, respectively.

To estimate the external forces and moments of *X*, *Y*, *Z*, *K*, *M*, and *N* in the dynamic model, these variables were modeled as a third-order Gauss-Markov (Eqs. (1)–(6)). This process was used to model the movement of the ship, with the assumption that the actual speed and direction of the current are considerably unknown and constant. It is also widely used as a black box model in signal processing when the characteristics of the prior time history are unknown [16].

$$\dddot{X} = w_X(t) \tag{1}$$

$$\dddot{Y} = w_Y(t) \tag{2}$$

$$\dddot{Z} = w_Z(t) \tag{3}$$

$$\dddot{K} = w_K(t) \tag{4}$$

$$\dddot{M} = w_M(t) \tag{5}$$

$$\dddot{N} = w_N(t) \tag{6}$$

where $w_{X,Y,Z,K,M,N}(t)$ is the white noise.

Based on this study, 30 variables were estimated by using the UKF in the conducted sensor fusion, which consisted of six

**Table 1**
Error characteristics of the simulated IMU.

| Parameters | Gyroscope (Angular Rates) | Accelerometer (Specific Forces) |
|---|---|---|
| Rate Noise Spectral Density | 0.01°/s | 300 μg |
| Low Pass Filter Response | 5–250 Hz | 5–260 Hz |
| Output Data Rate | 4–8000 Hz | 4–4000 Hz |

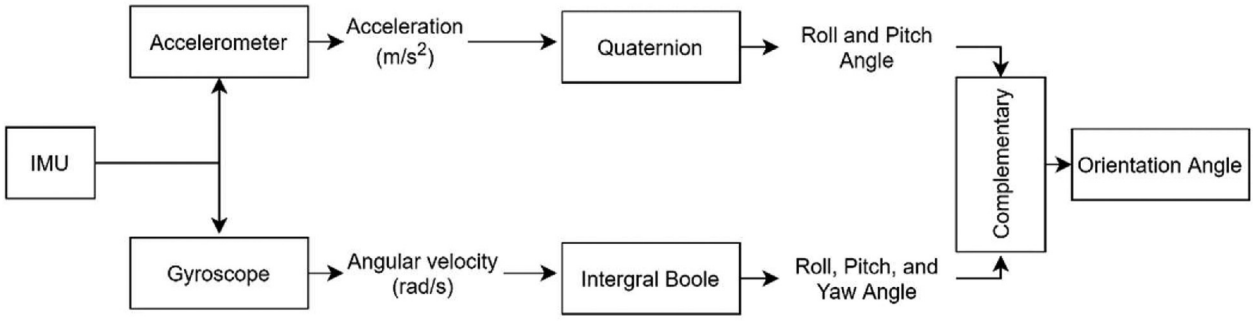


**Fig. 2.** A Phase of IMU sensor orientation angle (attitude) calculation (modified from Ref. [14]).

**Table 2**
Input data format.

| | Variables | Symbols | Units |
|---|---|---|---|
| GPS Data | Time | $t_{GPS}$ | s |
| | $X$ | $X$ | m |
| | $Y$ | $Y$ | m |
| | $Z$ | $Z$ | m |
| IMU Data | Time | $t_{IMU}$ | s |
| | Roll | $\phi$ | rad |
| | Pitch | $\theta$ | rad |
| | Yaw | $\psi$ | rad |
| | roll-rate | $P$ | rad/s |
| | pitch-rate | $Q$ | rad/s |
| | yaw-rate | $R$ | rad/s |

**Table 4**
The i-Boat dynamic model.

| Variable | Modeled as |
|---|---|
| $\dot{u}$ | $\frac{X-(m+m_x)qw+(m+m_x)rv}{(m+m_x)}$ |
| $\dot{v}$ | $\frac{Y-(m+m_y)ru+(m+m_y)pw}{(m+m_y)}$ |
| $\dot{w}$ | $\frac{Z-(m+m_z)pv+(m+m_z)qu}{(m+m_z)}$ |
| $\dot{p}$ | $\frac{K-(I_{zz}-I_{yy})qr}{(I_{xx}+J_{xx})}$ |
| $\dot{q}$ | $\frac{M-(I_{xx}-I_{zz})pr}{(I_{yy}+J_{yy})}$ |
| $\dot{r}$ | $\frac{N-(I_{yy}-I_{xx})pq}{(I_{zz}+J_{zz})}$ |

kinematic, six dynamic, and 18 external force variables, respectively. Hence the state vector can be written as follows:

$$\mathbf{x}_k = \left[x\, y\, z\, \varphi\, \theta\, \psi\, u\, v\, p\, q\, r\, X\, \dot{X}\, \ddot{X}\, Y\, \dot{Y}\, \ddot{Y}\, Z\, \dot{Z}\, \ddot{Z}\, K\, \dot{K}\, \ddot{K}\, M\, \dot{M}\, \ddot{M}\, N\, \dot{N}\, \ddot{N}\right]^{\mathrm{T}} \quad (7)$$

and the measurement model is as follows,

$$\boldsymbol{z}_k = \boldsymbol{H} \times \boldsymbol{x}_k \quad (8)$$

where $\boldsymbol{H}$ is a measurement matrix with dimension $n \times 30$, and $n$ is the number of measurement data. Due to these equations are still in continuous form, discretization is needed before the performance of the UKF simulation. This was conducted using the forward finite difference method (Eq. (9)) since the UKF represents a one-step estimation.

$$\frac{\mathrm{d}u}{\mathrm{d}t} = \frac{u_{k+1}-u_i}{\Delta t}\,\frac{\mathrm{d}u}{\mathrm{d}t} = \frac{u_{k+1}-u_i}{\Delta t} \quad (9)$$

Using Eq. (10), the discretization of variable $\dot{z}$ in Table 3 was obtained as follows:

$$\begin{aligned} z_{k+1} &= \Delta t(u_k\,(-\sin\theta_k) + v_k\cos\theta_k\ \sin\varphi_k + w_k\cos\theta_k\cos\varphi_k) \\ &\quad + z_k z_{k+1} = \Delta t(u_k\,(-\sin\theta_k) + v_k\cos\theta_k\ \sin\varphi_k \\ &\quad + w_k\cos\theta_k\cos\varphi_k) + z_k \end{aligned} \quad (10)$$

The mathematical model (see Tables 3 and 4) indicates the nonlinear system. Hence it is necessary to be carefully treated in the design of the Kalman filter because using Standard Kalman Filter to handle the nonlinear system may provide a solution far from optimal [1,17]. This study solved this nonlinear system using the UKF algorithms, which only used a linearization approach compared to the Extended Kalman Filter (EKF), which indicated that direct linearization was unnecessary. The UKF algorithm is described in Fig. 3.

In Fig. 3, $\widehat{\boldsymbol{x}}_0$ is the initial state vector, $P_0$ is the initial covariance error, $X_i$ is the sigma point, $W_i$ is the weight, UT is the unscented transform, K is the Kalman Gain, $k$ is the epoch time $k$th, $f(X_i)$ is the

**Table 3**
The i-Boat kinematic model.

| Variable | Modeled as |
|---|---|
| $\dot{x}$ | $u\cos\psi\cos\theta + v\,(-\sin\psi\cos\phi + \cos\psi\sin\theta\sin\phi) + w\,(\sin\psi\sin\phi + \cos\psi\cos\phi\sin\theta)$ |
| $\dot{y}$ | $u\sin\psi\cos\theta + v\,(\cos\psi\cos\phi + \sin\phi\sin\theta\sin\psi) + w\,(-\cos\psi\sin\phi + \sin\theta\sin\psi\cos\phi)$ |
| $\dot{z}$ | $u\,(-\sin\theta) + v\cos\theta\sin\phi + w\cos\theta\cos\phi$ |
| $\dot{\phi}$ | $p + q\tan\theta\sin\phi + r\tan\theta\cos\phi$ |
| $\dot{\theta}$ | $q\cos\phi + r\,(-\sin\phi)$ |
| $\dot{\psi}$ | $q\left(\frac{\sin\phi}{\cos\theta}\right) + r\left(\frac{\cos\phi}{\cos\theta}\right)$ |

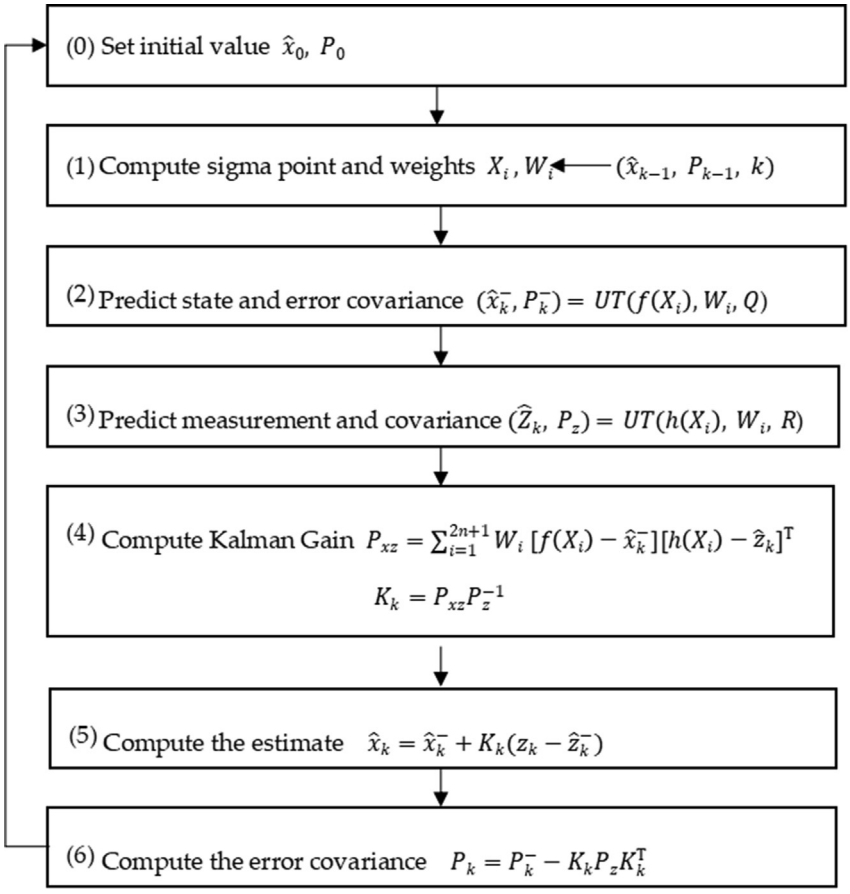


**Fig. 3.** The UKF algorithm.

function of the state vector, $Q$ is the covariance of the process, $R$ is the covariance of measurement, and $\mathbf{z}$ is the measurement vector.

Based on Fig. 3, the UKF initiation stage began by determining the initial value of the state vector ($\hat{\boldsymbol{x}}_0$) and covariance error ($P_0$). This was subsequently computed with a set of $2n + 1$ weighted points (Sigma points), where $n$ is the number of the system vector $\boldsymbol{x}$. These sigma points became the input for the unscented transform process during the state prediction. In this study, the sigma points were calculated using the nearest SPD decomposition to overcome the unstable system caused by the covariance matrix, which turned into an indefinite positive. Moreover, the nearest SPD minimized the difference of the Frobenius norm to determine the nearest matrix [18]. The whole Sigma points were then propagated through the nonlinear dynamic model, predicting the system's next state by assigning weights to each position. The algorithm subsequently estimated the optimal next state through the evaluation of the Minimum Mean Square Error (MMSE) of the GPS and IMU measurements/predictions. This led to the systematic update of the matrix to iterate the system and reduce the error covariance.

This simulation used non-dimensional data by normalizing the variables according to the rules in the Prime I System [15]. According to Table 5, each variable in both dynamic and kinematic models was also normalized. This further led to a variable with no units (non-dimensional), ensuring an easier calculation process during the UKF simulations. The normalization process required an i-Boat dimensional data, as stated in Table 5.

## 3. Result and analysis

In this study, two simulations of the GPS and IMU sensor fusion were analyzed. Also, an experiment with the module of the i-Boat trajectory tracking and the raw measurements process for the IMU and GPS sensors were carried out. According to Fig. 1, the rudder was found to drive the i-Boat because of supporting the designed trajectory. The different error types, including the Gaussian model (mean 0 and variance 1) and random noise, were also induced in the sensor fusion simulation to represent a real environmental condition closely. Furthermore, the program was implemented in

**Table 5**
The i-Boat parameters.

| Name | Size |
|---|---|
| USV length (L) | 4.70 m |
| USV width (B) | 2.08 m |
| Ship depth (T) | 0.3 m |
| Mass (m) | 510 kg |
| Velocity (U) | 15 knot (max) |

MATLAB R2017a. The two simulations performed to illustrate the performance of the proposed UKF algorithm were Scenarios I and II, respectively. Scenario I was conducted using the whole of the i-Boat measurement data, which contained nine parameters, namely $x$, $y$, $z$, roll, pitch, yaw, roll-rate, pitch-rate, and yaw-rate. Additionally, the UKF is known to provide reliable state estimation in the presence of both unknown process noise and slight measurement data [19]. This led to Scenario II, which was carried out by excluding the attitude measurement data.

The estimation of UKF provided the trajectory of USV in the horizontal plane (Fig. 4), where the results in Scenario II (green line) generally coincide with the measurement data (blue line). Meanwhile, the UKF estimation in Scenario I is represented by the red line, indicating the occurrence of several significant deviations from the measurement data.

The accuracy of the estimation was obtained by calculating the RMSE towards measurement data. This value and the maximum residue from each variable are shown in Table 6, which indicated that the maximum residue was the biggest absolute difference value from the estimation and measurement data.

Based on Scenario I, the RMSE value showed that the error estimations were 0.128 m, 0.027 rad, and 0.045 rad/s for the position, attitude, and angular rate, respectively. Meanwhile, the estimates of Scenario II were 0.062 m and 0.008 rad/s for position and angular rate, respectively. In this study, the position error from the UKF estimation was better categorized than the 3 DOF report, using both the kinematic and dynamic models developed by Ref. [20]. This led to an estimated value of 1.12 m, where the UKF simulation in Scenario II produced a more accurate estimation than in Scenario I. The comparison of each UKF estimation variable in Scenario I and II is shown explicitly in Fig. 5. Based on the comparison chart, the estimation in Scenario I had several significant deviations from the measurement data. A similar occurrence was also observed in the maximum residue value obtained from Scenario I, which was bigger than in Scenario II. Although the conventional UKF algorithm was able to reduce the raw sensor measurement errors, the estimation of the USV position still provided lower accuracy at 30%, compared to the modified model [8].

Previously, Cahyadi et al. [21] had also performed fusion using Geopointer software based on the EKF algorithm on i-Boat navigation. In this study, UKF's performance in sensor fusion has been compared with that of processing by Geopointer Software in estimating position, speed, and attitude. The comparison shows that the UKF provides positioning accuracy of up to 0.040 m, while the EKF can only achieve an accuracy of 0.413 m.

**Table 6**
RMSE and maximum residual in Scenarios I and II.

| Variable | RMSE UKF | | Maximum residual | |
|---|---|---|---|---|
| | Scenario I | Scenario II | Scenario I | Scenario II |
| $x$ (m) | 0.0741 | 0.0307 | 1.9724 | 0.9670 |
| $y$ (m) | 0.0741 | 0.0260 | 1.9724 | 0.5468 |
| $z$ (m) | 0.0741 | 0.0476 | 1.9724 | 0.8410 |
| $\phi$ (rad) | 0.0158 | – | 0.4197 | – |
| $\theta$ (rad) | 0.0158 | – | 0.4197 | – |
| $\psi$ (rad) | 0.0158 | – | 0.4197 | – |
| $p$ (rad/s) | 0.0259 | 0.0028 | 0.6890 | 0.0167 |
| $q$ (rad/s) | 0.0259 | 0.0080 | 0.6890 | 0.0778 |
| $r$ (rad/s) | 0.0259 | 0.0003 | 0.6890 | 0.0023 |

Based on the residual value, the norm error of 3D positioning was calculated as $\Delta p = \sqrt{\Delta x^2 + \Delta y^2 + \Delta z^2}$. Fig. 6 shows the comparison of this error position from Scenarios I and II, which indicates that Scenario II provided a smaller norm error than Scenario I. However, this was extremely larger during the initial time, and the maximum norm errors of the 3D positioning for Scenarios II and I were 0.231 and 0.727 m, respectively.

## 4. Discussion

The results of the UKF simulation in both scenarios show an anomaly compared to most Kalman Filter researches. In Section 3, Scenario II is more accurate than Scenario I. This study conducts mathematical justification to prove that the presence of attitude measurement data caused a decrease in fusion accuracy. More accurate filtering is obtained when the covariance matrix $\boldsymbol{P}$ is smaller [22]. Hence the comparison between covariance matrix $\boldsymbol{P}$ in Scenario I and II using Loewner order [23], which is defined through the cone of positive semidefinite matrices $Sym^{+}(n)$ as follows:

$$\boldsymbol{A}, \boldsymbol{B} \in Sym\ (\boldsymbol{n})\ : \boldsymbol{A} \geq \boldsymbol{B} \in Sym^{+}(\boldsymbol{n}),$$

if and only if $\boldsymbol{A} - \boldsymbol{B}$ is positive semidefinite.

The analysis shows that $\boldsymbol{P}_{\text{Scenario II}} - \boldsymbol{P}_{\text{Scenario I}}$ is not positive definite. Hence, we got that $\boldsymbol{P}_{\text{Scenario II}} \leq \boldsymbol{P}_{\text{Scenario I}}$ is tenable. Since the error covariance matrix $\boldsymbol{P}$ is proportional to the Kalman gain

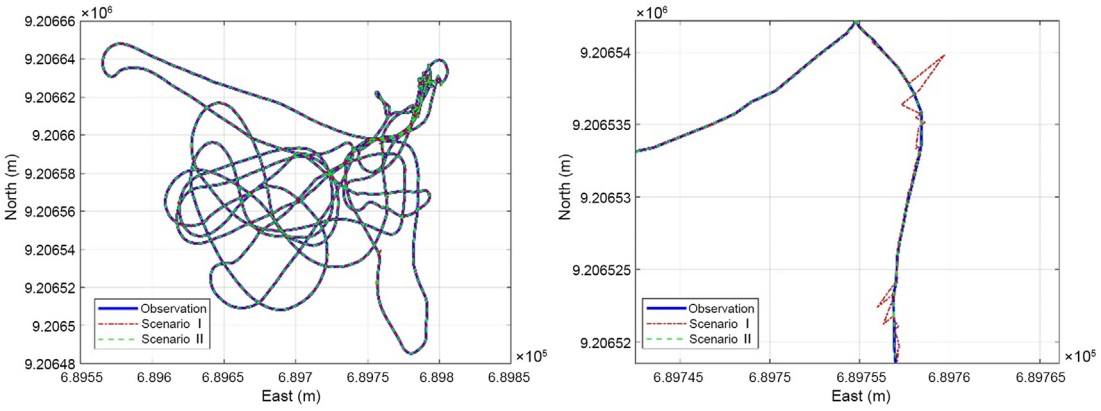


**Fig. 4.** Trajectory estimation based on Scenarios I and II.

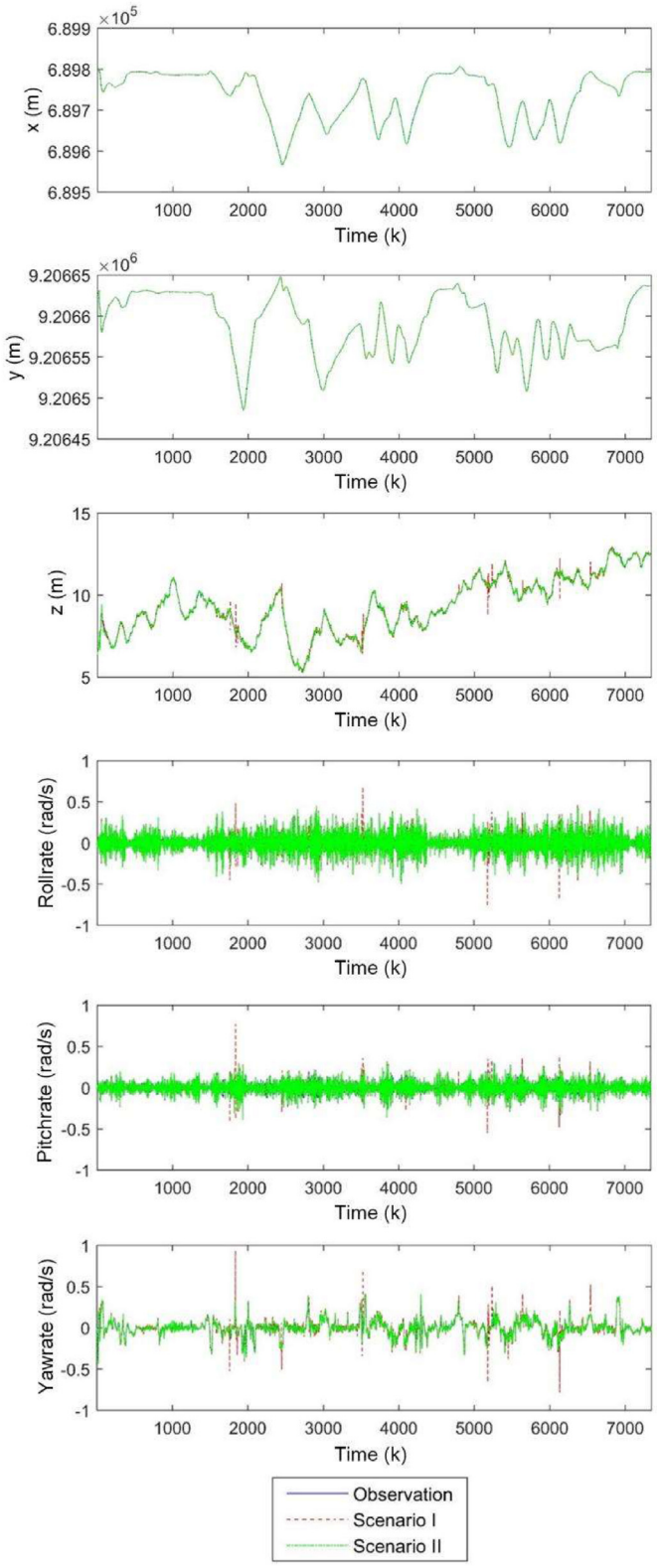


**Fig. 5.** Comparison of UKF estimation results from Scenario I and Scenario II. Time $k$ is the epoch at the $k$th time.

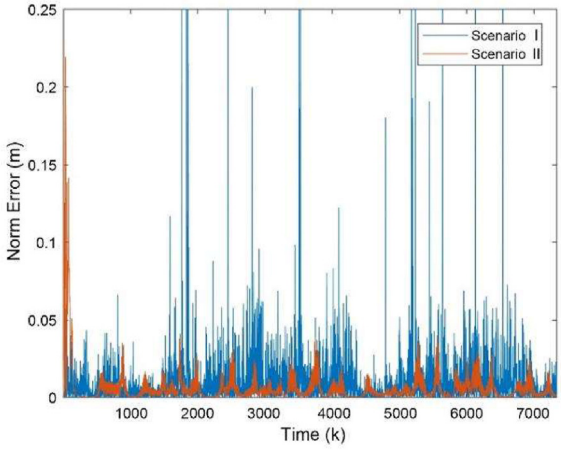


**Fig. 6.** Comparison of UKF norm error from Scenario I and Scenario II. Time k is the epoch at the kth time, and norm error is the deviation of 3D position in meters.

($K$), therefore $K_{\text{Scenario II}} \leq K_{\text{Scenario I}}$. This property indicates that the influence of the measurement model on UKF is reduced, but the influence of the state equation on UKF is increased when Scenario II is simulated to estimate the epoch $t_{k+1}$. However, the effect of the state equation on UKF is increased when Scenario II is simulated to estimate the epoch $t_{k+1}$. These anomalies were because the simulation with more measurement data should be used to provide a better estimation. The anomaly detected in this study was caused by several factors, such as the limitation of the UKF algorithm [24], a less suitable parameter model [19], or a very large variance of measurement data. The i-Boat simulation was conducted in Madura Strait, and the water showed a relatively small range (0.28–3.54 cm/s) in the northeast, east, and southeast directions [25]. Moreover, the wave characteristics showed a tendency to become bigger weekly, affecting the stability of USV during the operation. The bigger variant of attitude data was also caused by noise accumulation during the accelerometer and gyroscope measurements [19]. Therefore, the drift value in the data was bigger with time. When the attitude data was included in the simulation, a decrease was observed in the accuracy shown by the larger RMSE in Scenario I. This attitude data was obtained from the processing by IMU sensor, not direct measurements. Angular velocity and specific force data were also processed using Boolean integrals to obtain the attitude parameters (Fig. 2). When the angular velocity had a large noise, error propagation was observed in that process. The propagation at the IMU was influenced by the scale factor and cross-coupling errors that relied on the USV dynamics [6].

The UKF simulation was conducted with different combinations of data attitude to validate the hypothesis that this factor (data attitude) had a large noise. Scenario A: using pitch and yaw data measurements; Scenario B: using roll and yaw data measurements; Scenario C: using roll and pitch data measurements; Scenario D: using roll data measurement; Scenario E: using $\theta$ pitch measurement; Scenario F: using yaw data measurement.

These six simulations produced trajectory estimation and RMSE value, as shown in Fig. 7 and Table 7, respectively. Based on Fig. 7, the yaw measurement data was included in the UKF simulation, providing significant deviation in several parts of the estimation

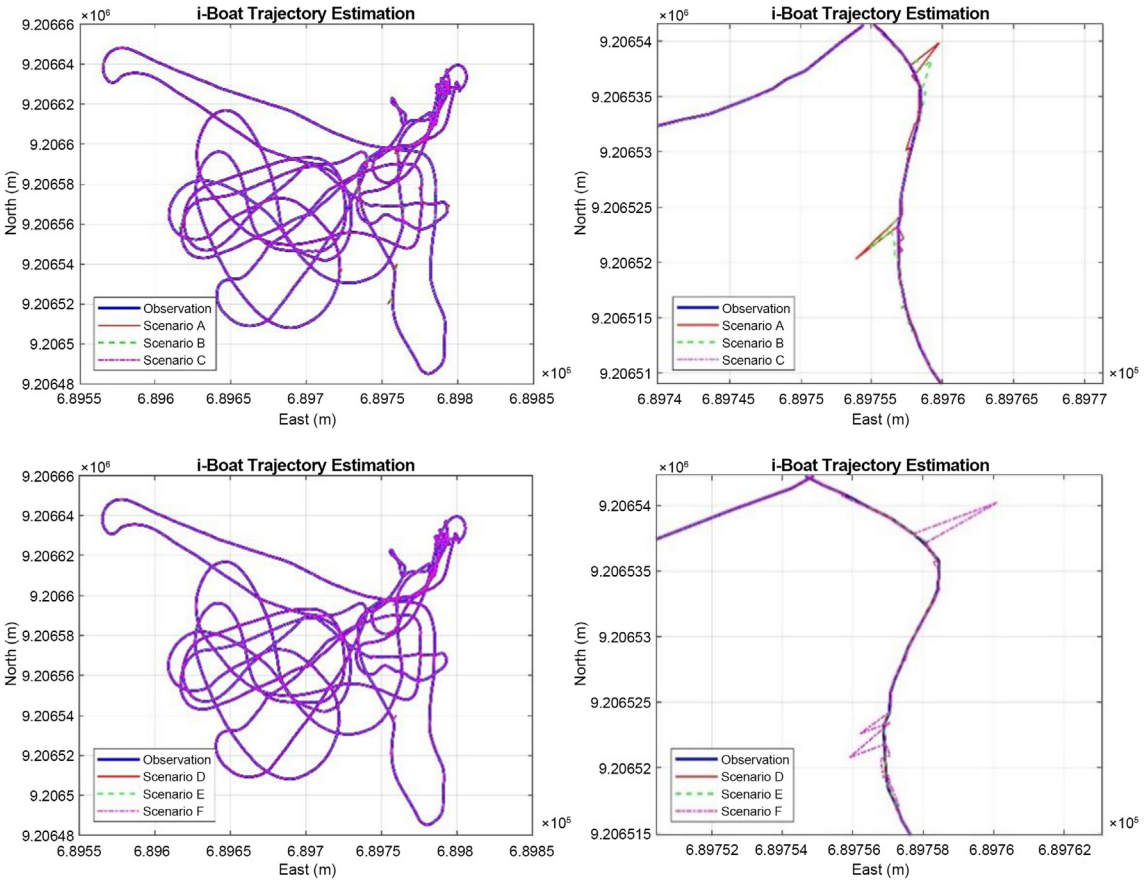


**Fig. 7.** Comparison of UKF estimation results from modification scenario.

trajectory. However, better estimation was produced by excluding this measurement data from the simulation.

Table 7 shows that the A and B Scenarios produced a bigger RMSE and residue value, compared to C. This was because the appearance of yaw data differentiated the three scenarios. The use of eight input data measurements (Scenarios A, B, C) in this simulation produced a bigger RMSE than those without yaw parameters. This indicated that the yaw data had the highest noise compared to the other attitude parameters. Meanwhile, the use of seven input measurement data (Scenarios D, E, and F) showed that Scenario F had the highest RMSE value compared to D and E. This indicated that there was a bigger noise in the yaw data measurement. The previous studies conducted the Scenario measurement of GPS and Inertial Navigation System (INS) integration showed that the yaw and roll data had bigger noises than the pitch [26].

An analysis of the attitude data characteristics was also carried out to identify the cause of the very extreme yaw angle residue in Scenario I. This was performed in a time series by separating the positive and negative angle data. Based on the direction of rotational movement, this separation was subsequently conducted clockwise and counterclockwise (rotations on the positive and negative axes) [27]. Furthermore, the moving mean value of each parameter was calculated in every 100 data. The mean motion also suppresses the noise in the unstable time series data, especially where the variance was sufficiently large to exceed the threshold value [28]. According to Fig. 8, several measurement data (blue line) are observed outside the area bounded by the positive and negative-moving mean (green lines). These were considered outliers due to causing a larger data variance.

The RMSE calculation was then conducted from several outliers to the nearest moving mean value to determine noise accumulation characteristics in the attitude data. Table 8 also shows that the yaw has the largest RMSE value compared to the other attitude data, indicating that it contains larger noise than the pitch and roll.

This study simulated the integrated GPS/INS measurement [29], providing a larger RMSE in the yaw and roll data compared to the pitch. The yaw angle in vehicle movement was also the most undetectable state since the inclination in the z-axis measurement required a longer stability time [1]. In future studies, more sensors should be combined for precise i-Boat navigation.

**Table 7**
RMSE of UKF estimation results from modification scenario.

| Simulation | RMSE | |
|---|---|---|
| | Position (m) | Angular velocity (rad/s) |
| A | 0.136 | 0.048 |
| B | 0.139 | 0.049 |
| C | 0.047 | 0.016 |
| D | 0.049 | 0.017 |
| E | 0.040 | 0.014 |
| F | 0.121 | 0.042 |

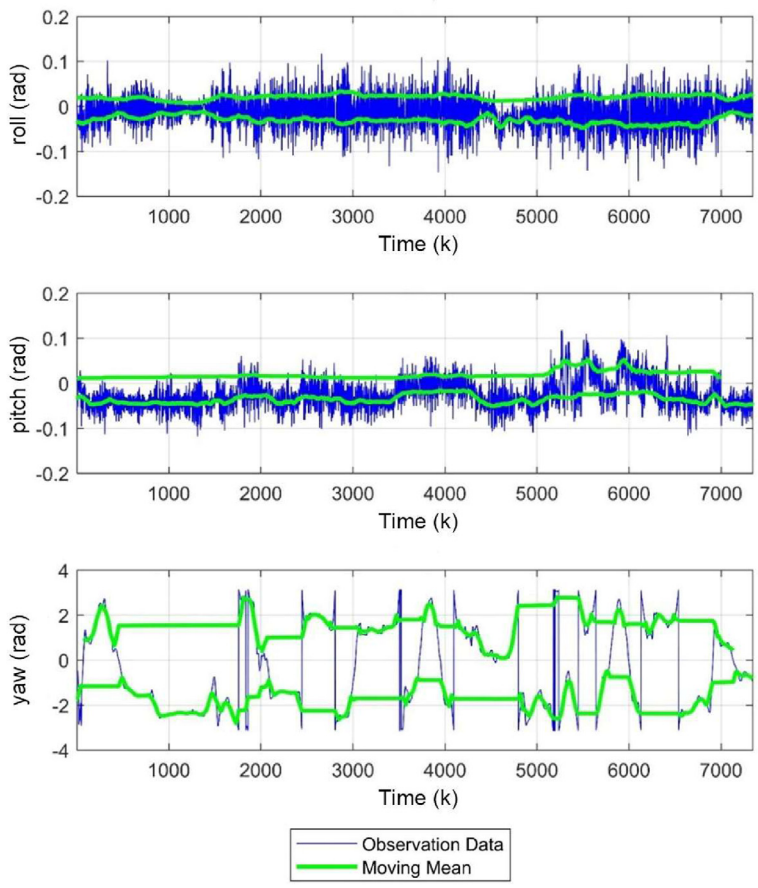


**Fig. 8.** Moving mean of attitude data.

**Table 8**
Data outlier characteristic.

| Euler angles | Number of data | RMSE (rad) |
|---|---|---|
| $\phi$ | 3127 | 0.025215 |
| $\theta$ | 3429 | 0.020889 |
| yaw | 3682 | 0.403571 |

## 5. Conclusions

The procedures in this study were simulated to compute GPS and IMU sensor fusion for i-Boat navigation using a limit algorithm in the 6 DOF. Two conducted Scenarios were also observed in the simulations, namely attitude measurement data inclusion and exclusion. According to the analysis, the obtained 3D position accuracy were 0.128 and 0.062 m for Scenarios I and II, respectively. The increased accuracy in Scenario II has been obtained because the simulation was carried out without involving attitude measurement data that contains large noise. The RMSE was becoming worse after the application of measurement data towards Scenario I. Thus, in Scenario II, the filter becomes more stable in the estimation according to the reference trajectory. The large noise in the measurement data is caused by the limit in the IMU sensor to conduct measurements in high-dynamic shallow seas. Future studies are expected to utilize several dynamical models with more suitable environmental conditions. They should also enhance the conventional UKF algorithm, as well as verify and correct the associated sensor noise in real-time.

## Author contributions

Conceptualization (MC and TA), Data curation (RM and RE), Formal analysis (MC and TA), Funding acquisition (RM), Investigation (RM), Methodology (TA), Writing: original draft (RE) and review/editing (MC).

## Conflicts of interest

The authors declare no conflict of interest.

## Acknowledgments

The authors are grateful to the i-Boat ITS Team, DRPM ITS Indonesia, and World-Class Professor Program (Ministry of Higher Education, Research, and Technology, Indonesia) for the data and financial support of this study.

## References

[1] G. Xia, G. Wang, INS/GNSS tightly-coupled integration using quaternion-based AUPF for USV, Sensors 16 (2016) 1215.
[2] S.G. Jin, K. Su, PPP models and performances from single- to quad-frequency BDS observations, Satellite Navigation 1 (2020) 1–13.
[3] N.A. Famiglietti, G. Cecere, C. Grasso, A. Memmolo, A. Vicari, A test on the potential of a low-cost unmanned aerial vehicle RTK/PPK solution for precision positioning, Sensors 21 (2021) 3882.
[4] H. Yoon, H. Seok, C. Lim, B. Park, An online SBAS Service to improve drone navigation performance in high-elevation masked areas, Sensors 20 (2020) 3047.

[5] X. Meng, H. Wang, B. Liu, A robust vehicle localization approach based on GNSS/IMU/DMI/LiDAR sensor fusion for autonomous vehicles, Sensors 17 (2017) 2140.
[6] P.D. Groves, Principles of GNSS, Inertial, and Multisensor Integrated Navigation Systems, Artech house, Boston, USA, 2013, pp. 7–117.
[7] M.N. Cahyadi, I. Rwabudandi, Integration of GNSS-IMU for increasing the observation accuracy in condensed areas (infrastructure and forest canopies), E3S Web Conf. 94 (2019), 03015.
[8] W. Liu, Y. Liu, R. Bucknall, A robust localization method for unmanned surface vehicle (USV) navigation using fuzzy adaptive Kalman filtering, IEEE Access 7 (2019) 46071–46083.
[9] M.Z. Guo, C. Guo, C. Zhang, SINS/GNSS-Integrated navigation of surface vessels based on various nonlinear Kalman filters and large ship dynamics, J. Electr. Eng. Technol. 16 (2021) 531–546.
[10] Y.J. Chen, X. Yuan, S.L. Du, C. Song, Research on ship automatic modeling and identification system, in: Proceedings of the 2017 2nd International Conference on Mechatronics and Information Technology (ICMIT 2017), Xi'an, 2017.
[11] U.I. Taz, M. Mulk, J. Falzarano, Complete six-degrees-of-freedom nonlinear ship rolling motion, J. Offshore Mech. Arctic Eng. 116 (1994) 191–201.
[12] Shen C, Xiong Y, Zhao D, Wang C, Cao H, Song X, Tang J, Liu J. Multi-rate strong tracking square-root cubature Kalman filter for MEMS-INS/GPS/polarization compass integrated navigation system. Mechanical Systems and Signal.
[13] C. Shen, Y. Zhang, X. Guo, X. Chen, H. Cao, J. Tang, J. Li, J. Liu, Seamless GPS/inertial navigation system based on self-learning square-root cubature Kalman filter, IEEE Trans. Ind. Electron. 68 (1) (2020) 4.
[14] A. Nurhakim, H.M. Saputra, N. Ismail, Complementary of quaternion method and Boole's rule on IMU sensor to cal-culate orientation angle of Stewart Platform, Proceedings of the J. Phys. Conf. Ser. 1402 (3) (2019) 033106. Bali, Indonesia.
[15] T.I. Fossen, Handbook of Marine Craft Hydrodynamics and Motion Control, John Wiley & Sons, New York, USA, 2011, pp. 15–41.
[16] H. Yoon, K. Rhee, Identification of hydrodynamic coefficients in ship maneuvering equations of motion by estimation-before-modeling technique, Ocean. Eng. 30 (2003) 2379–2404.
[17] S. Konatowski, A.T. Pieni, A comparison of estimation accuracy by the use of KF, EKF & UKF filters, WIT Trans. Model. Simul 46 (2007).
[18] Nicholas J. Higham, Computing a nearest symmetric positive semidefinite matrix, Lin. Algebra Appl. 103 (1988) 103–118.
[19] B. Zheng, P. Fu, B. Li, X. Yuan, A robust adaptive unscented Kalman filter for nonlinear estimation with uncertain noise covariance, Sensors 18 (2018) 808.
[20] J.H. Ryu, G. Gankhuyag, K.T. Chong, Navigation system heading and position accuracy improvement through GPS and INS data fusion, J. Sens. 2016 (2016) 6.
[21] M.N. Cahyadi, T. Asfihani, R. Mardiyanto, R. Erfianti, Loosely coupled GNSS and IMU integration for accurate i-Boat horizontal navigation, Int. J. Geoinf 18 (3) (2022) 111–122.
[22] Y. Li, Q. Gui, S. Han, Y. Gu, Tikhonov regularized Kalman filter and its applications in autonomous orbit determination of BDS, WSEAS Trans. Math. 16 (2017) 187–196.
[23] Burgeth, B.; Kleefeld, A. Morphology for color images via Loewner order for matrix fields. In International Symposium on Mathematical Morphology and its Applications to Signal and Image Processing, Springer, Berlin, Heidelb.
[24] A.E. Pelevin, Identification of vehicle model parameters under external disturbances, Gyroscopy Navig 6 (2015) 143–148.
[25] Harbor weather forecast, maritime meteorological center, meteorology climatology and geophysics council (BMKG) Indonesia. https://maritim.bmkg.go.id/area/pelabuhan/?id=7 accessed on 12 January 2021.
[26] Asfora, B.A.; dos Santos, D.A. Comparison of filtering methods for stereo visual-inertial navigation of multirotor aerial vehicles. In Proceedings of the 24th ABCM International Congress of Mechanical Engineering, Curitiba.
[27] LSM303D datasheet, Available online: https://www.pololu.com/file/0J703/LSM303D.pdf. accessed on 8 Januari 2021.
[28] S. Han, Z. Meng, O. Omisore, T. Akinyemi, Y. Yan, Random error reduction algorithms for MEMS inertial sensor accuracy improvement—a review, Micromachines 11 (2020) 1021.
[29] L. Chang, X. Niu, T. Liu, J. Tang, C. Qian, GNSS/INS/LiDAR-SLAM integrated navigation system based on graph optimization, Rem. Sens. 11 (2019) 1009.

**Mokhamad Nur Cahyadi** have earned a Ph.D. from the Natural History Laboratory of Hokkaido University, Japan, in 2014. His current daily life is as a lecturer at the Department of Geomatics Engineering ITS for undergraduate and master's study programs. He is also the Deputy Head of the Marine-Earth Science and Technology Research Center, ITS Directorate of Research and Community Service. His research fields are the development of Low-cost GNSS and ionospheric disturbance analysis (TEC), which are applied in the field of geomatics, such as land parcel measurement, mapping using UAV, mapping of regional boundaries, and hydrographic surveys.

**Tahiyatul Asfihani** is currently a Lecturer at the Department of Mathematics, Sepuluh Nopember Institute of Technology. She received a Dr. degree in marine engineering from the Sepuluh Nopember Institute of Technology in 2019. She gained working experience in shipping and optimization control.

**Ronny Mardiyanto** received an M.T. degree in electrical engineering from Bandung Institute of Technology in 2006 and a Ph.D. degree in Electrical Engineering from Saga University, Japan, in 2011. He is currently a Lecturer with the Department of Electrical Engineering, Sepuluh Nopember Institute of Technology. His research focuses on Robot, Vision, Biomedical, electronic, and UAV Technology. He is currently working on the project of autonomous navigation for unmanned surface vehicles.

**Risa Erfianti** is a master student at Geomatics Engineering, Sepuluh Nopember Institute of Technology. In her undergraduate study, she is working on few research topic, such as LiDAR data processing to create Digital Terrain Model, satellite imagery for monitoring air quality, and designing webGIS for mapping the vulnerability of COVID-19 cases. Currently, she focuses on studying the development of GNSS application with robust multi-sensor data fusion algorithms.